Molecular Beam Chemistry. Formation of Phenyl Cations from C_6H_5X Molecules

S. A. Safron,* G. A. King,† and R. C. Horvat

Contribution from the Chemistry Department, Florida State University, Tallahassee, Florida 32306. *Received April 30, 1981*

Abstract: Reactive scattering experiments between Cs^+ and C_6H_5X molecules with X = F, Br, I, and NO_2 are reported and the results compared to previous experiments with X = Cl. The formation of the phenyl cation is discussed in terms of the intersection of two potential energy surfaces, one involving the interaction between Cs^+ and covalent C_6H_5X and the other involving the interaction between Cs^+ and an excited ionic $C_6H_5{}^+X^-$ molecule. A simple "knockout" model gives a realistic picture for this reaction and is employed to interpret the measured energy distributions and appearance potentials. Implications of this work for ion intermediates in solution are also discussed.

The phenyl cation is the well-known ion observed principally in the mass spectrum of substituted benzene compounds. The several quantum chemical calculations performed on $C_6H_5^+$ have shown that its most stable electronic configuration is the singlet corresponding to the removal of the lone σ electron of the phenyl radical.[1-3] The geometry of this species is distorted from the hexagonal shape of benzene by a widening of the C-C^+-C bond angle from 120° to ~145°.[2] Reactions of $C_6H_5^+$ in the gas phase studied by ICR[4] have suggested that it is a strong electrophile "exhibiting both carboniumlike and carbenelike reactivity", which is consistent with this electronic configuration.

In solution the phenyl cation has only rarely been implicated as an intermediate species,[5] unlike such cations as benzyl and *tert*-butyl which have often been invoked in reaction mechanisms and even directly observed spectroscopically.[6] Like the phenyl cation these ions are also prominent in the appropriate mass spectra and engage in similar gas-phase reactions.[7] The dipole moments of molecules such as benzyl chloride, *tert*-butyl chloride, and chlorobenzene are sufficiently similar (all ~ 2 D)[8] that the respective C-Cl bonds probably are similarly covalent.[9] Differences do arise in the bond energies of these compounds so that the gas-phase dissociation RCl → $R^+ + Cl^-$ requires the input of about 2 eV more energy for R = phenyl than for R = benzyl or for R = *tert*-butyl.[10] Whether such a dissociative process can also take place in solution to any appreciable extent depends not only on the solvation energy of the R^+ and Cl^- ions but also on the extent of stabilization that solvation can provide during the formation of the ion pair. That is, the process should be represented as RCl → R^+Cl^- → $R^+ + Cl^-$, where the first step is the formation of the ion pair from the covalently bonded RCl.

In previous molecular beam investigations of the reactions

$$RCl + Cs^+ \rightarrow R^+ + CsCl \qquad (1)$$

where R is benzyl[11] or *tert*-butyl,[12] the experimental results showed that the products were scattered in the forward direction to a very significant extent, particularly in the *tert*-butyl case. Model potential energy surface calculations[13] indicate that this result is to be expected for reactions governed by potential energy surfaces which are of the "early downhill" or attractive type. Thus even though the reactions for both benzyl and *tert*-butyl chlorides are *endoergic* by ~2 eV, one is led to the conclusion[14] that the energy barrier to reaction must be overcome *late* in the course of the process while the formation of the R^+Cl^- ion pair must occur *early* in the attractive entrance channel of the potential surface. While Cs^+ does not resemble the usual solvent molecule, it does interact with RCl in the same basic manner, electrostatically. Hence, there is the correlation with the solution behavior of these compounds: just as these molecules are able to form the ion pair electronic configuration under the influence of the Cs^+-RCl ion-dipole force at fairly long range, so are they able to form the ion-pair configuration under the influence of the weaker dipole-dipole forces with solvent molecules at close range.

In similar molecular beam experiments with R = phenyl,[15] the scattered products were found essentially exclusively backward scattered. The corresponding conclusion here is that the potential energy surfaces are "repulsive", and hence that the ion pair is formed *as* the energy barrier is being overcome or later. This again is consistent with the solution behavior of chlorobenzene in that at the usual solvent molecule–solute molecule interaction distances, the electrostatic forces are too weak to "induce" the formation of the ion pair even if they could provide sufficient solvation energy for the separated ions.

We report here further scattering experiments on the reactions of

$$Cs^+ + C_6H_5X \rightarrow CsX + C_6H_5^+ \qquad (2)$$

where X = F, Br, I, and NO_2. In addition, the fragmentation of $C_6H_5^+$ via

$$C_6H_5^+ \rightarrow C_4H_3^+ + C_2H_2 \qquad (3)$$

is also observed. The results are fairly well described by a simple model which is consistent with qualitative picture described above.

† NSF Undergraduate Research Participant.

(1) Evleth, E. M.; Horowitz, P. M. *J. Am. Chem. Soc.* **1971**, *93*, 5636-5639.
(2) Dill, J. D.; Schleyer, P. v. R.; Binkley, J. S.; Seeger, R.; Pople, J. A.; Haselback, E. *J. Am. Chem. Soc.* **1976**, *98*, 5428-5431.
(3) Dill, J. D.; Schleyer, P. v. R.; Pople, J. A. *J. Am. Chem. Soc.* **1977**, *99*, 1-8.
(4) For example, see: Speranza, M.; Sefick, M. D.; Henis, J. M. S.; Gaspar, P. P. *J. Am. Chem. Soc.* **1977**, *99*, 5583-5589.
(5) Swain, C. G.; Sheats, J. E.; Harbison, K. G. *J. Am. Chem. Soc.* **1975**, *97*, 783-790, present evidence for a singlet phenyl cation intermediate.
(6) For examples, see: Gould, E. S. "Mechanism and Structure in Organic Chemistry"; Holt, Rinehart and Winston: New York, 1959; and references cited therein.
(7) For examples, see: Abboud, J.-L. M.; Hehre, W. J.; Taft, R. W. *J. Am. Chem. Soc.* **1976**, *98*, 6072-6073 and references cited therein. Hiraoka, K.; Kebarle, P. *J. Am. Chem. Soc.* **1977**, *99*, 360-366.
(8) For example, see: Weast, R. C., Ed. "Handbook of Chemistry and Physics"; 51st ed.; Chemical Rubber Company: Cleveland, 1971; p E-51.
(9) Probably a better measure of ionic or covalent character is the nuclear quadrupole coupling constant. These are also similar for benzyl chloride, *tert*-butyl chloride, and chlorobenzene, being 67.25, 62.13, and 69.24 MHz, respectively. See: Lucken, E. "Nuclear Quadrupole Coupling Constants"; Academic Press: London, 1969; pp 169 and 185.
(10) From: Franklin, J. L.; Dillard, J. G.; Rosenstock, H. M.; Herron, J. T.; Draxl, K.; Field, F. H. "Ionization Energies, Appearance Potentials and Heats of Formation of Gaseous Positive Ions"; National Bureau of Standards: Washington, D.C., 1969. One can estimate $D_0(R^+-Cl^-)$ to be 6.5 eV for R = benzyl, 7.0 eV for R = *tert*-butyl, and 9.0 eV for R = phenyl.
(11) Safron, S. A.; Miller, G. D.; Rideout, F. A.; Horvat, R. C. *J. Chem. Phys.* **1976**, *64*, 5051-5064.
(12) Horvat, R. C.; Safron, S. A. *Chem. Phys. Lett.* **1980**, *69*, 177-181.
(13) For a review, see: Polanyi, J. C.; Schreiber, J. L. In "Physical Chemistry, VIA", Jost, W., Ed.; Academic Press: New York, 1974.
(14) One should always be cautious about extrapolating model calculations for small systems to larger ones. See, for example: Chapman, S. *J. Chem. Phys.* **1981**, *74*, 1001-1011.
(15) Horvat, R. C.; Miller, G. D.; Safron, S. A. *J. Am. Chem. Soc.* **1976**, *98*, 8274-8276.

0002-7863/81/1503-6333$01.25/0

Table I. ΔH° of Reaction and Appearance Potentials[a,b]

organic reactant	ΔH° (eq 2)	ΔH°_{calcd} (eq 2)[d]	AP-($C_6H_5^+$)	ΔH° (eq 2 + 3)	ΔH°_{calcd} (eq 2 + 3)[d]	AP-($C_4H_3^+$)
C_6H_5Cl[c]	3.6	4.7	5.9	7.7	7.2	9.0
C_6H_5Br	3.5	3.3	4.8	7.6	6.0	8.9
C_6H_5I	3.4	3.2	5.2	7.5	6.1	10.0
$C_6H_5NO_2$	3.5	4.6	6.0	7.6	7.7	10.1
C_6H_5F	4.4			8.5		

[a] All energies are in eV. The uncertainties in the measured AP's are estimated to be ±0.5 eV. [b] The ΔH°'s of reaction are calculated by using the gas phase ΔH°_f's of Cs^+ (4.74), CsCl (−2.71), CsI (−1.83), C_6H_5Cl (0.55), C_6H_5Br (1.04), C_6H_5I (1.61), $C_6H_5NO_2$ (0.65), $C_4H_3^+$ (13.3), and C_2H_2 (2.36) from ref 10. The ΔH°_f's of CsBr and CsF were estimated to be −2.26 and −3.53 eV, respectively. The ΔH°_f of $C_6H_5^+$ (11.57) was taken from Leung, Hei-Wun; Harrison, Alex G. *J. Am. Chem. Soc.* 1979, *101*, 3168-3173. The ΔH°_f of $CsNO_2$ (−2.72) was calculated from the D_0(Cs-NO_2) given by: Bagaratian, N.; Verkhoturov, E.; Ilyin, M.; Marakov, A.; Nikitin, D. *Adv. Mass Spectrom.* 1978, *7a*, 578-583. The ΔH°_f's of Cs (0.82) and NO_2 (0.34) are from ref 10. The precision of the ΔH°'s is estimated to be ±0.3 eV. [c] The results for C_6H_5Cl are taken from ref 15. The ΔH° values are corrected by using the newer value of ΔH°_f for $C_6H_5^+$ (above) rather than that reported in ref 10. [d] These ΔH° values are calculated from the AP's according to the Ideal Knockout Model as described in the text.

Experimental Section

The apparatus for these experiments is described in detail elsewhere.[11] Briefly it consists of a cylindrical main or scattering chamber with an attached, but separately pumped, detector chamber. The Cs^+ ion beam and the roughly thermal (~300 K) C_6H_5X beam sources are mounted from the rotatable lid of the main chamber. The beams intersect with a 90° angle directly under the center-of-rotation of the lid, the neutral beam being directed along the axis of rotation. Thus the plane in which the scattering is measured, defined by the Cs^+ beam and the detector axis, is perpendicular to the plane defined by the beams. The full range of accessible laboratory frame (LAB) scattering angles, Φ, is −90° to +90° with respect to the Cs^+ beam (directed along the detector axis at $\Phi = 0°$).

The detector itself is a quadrupole mass spectrometer with a channeltron electron multiplier operated in the pulse-counting mode. A stopping potential technique is employed for energy analysis of the product ions; the angular distribution of product ions is obtained directly from the total scattered intensity with the energy analyzer removed. These data are then combined to yield the usual center-of-mass (c.m.) Cartesian contour diagram or kinematic map of the scattering. Since the product intensities are quite low (typically in the range 1-100 counts/s) we take advantage of the (required) symmetry of the scattering about $\Phi = 0°$ to improve the signal-to-noise ratio by combining the data from positive and negative angles.[16] (This also forces the diagram to appear perfectly symmetric about the Cs^+ velocity vector.)

A simplifying feature of our reactive systems is that the Cs^+ velocities are very much larger than those of the C_6H_5X molecules. Hence, the relative velocity vector V is very nearly identical with the Cs^+ velocity vector, V_{Cs^+}. Thus, the principal smearing factors in these experiments are the angular width (~5° fwhm) and the translational energy width (~5% full width) of the Cs^+ beam.

Appearance potential energy measurements are made by varying the Cs^+ beam energy until the product ion just becomes detectable, ≳1 count/10 s, corresponding to an estimated cross section of $\sim 10^{-2}$ Å^2. Since cross sections for endoergic processes generally rise rapidly with increasing energy from threshold, we estimate our uncertainties at ~±0.5 eV. This is not especially good. However, the apparatus was designed primarily for the angular-energy distribution measurements.

Results

Table I lists the ΔH°'s of reaction for the formation of $C_6H_5^+$ (eq 2) and for the sum of eq 2 and eq 3 leading to the formation of $C_4H_3^+$. These are accompanied by the measured appearance potentials (AP) for each process, which do not appear to agree well. (However, see the Discussion section.) The cross section for the reaction with fluorobenzene was so small that no reliable AP for either $C_6H_5^+$ or $C_4H_3^+$ could be obtained, nor could angular or energy analysis data be obtained for reaction 2. For fluorobenzene the only result is that reactions 2 and 3 do appear to take place. For the other compounds the cross sections for eq 2 are estimated to be ~0.5 Å^2 at ~9 eV collision energy.

Typical energy analysis data are shown in Figure 1 for the reaction with iodobenzene. The LAB energy distributions $P(E_L)$ are obtained from the measured stopping curves $I(E_L)$ by differentiation since $I(E_L) = \int_{E_L}^{\infty} P(E_L)\, dE_L$.[11] The Cartesian contour

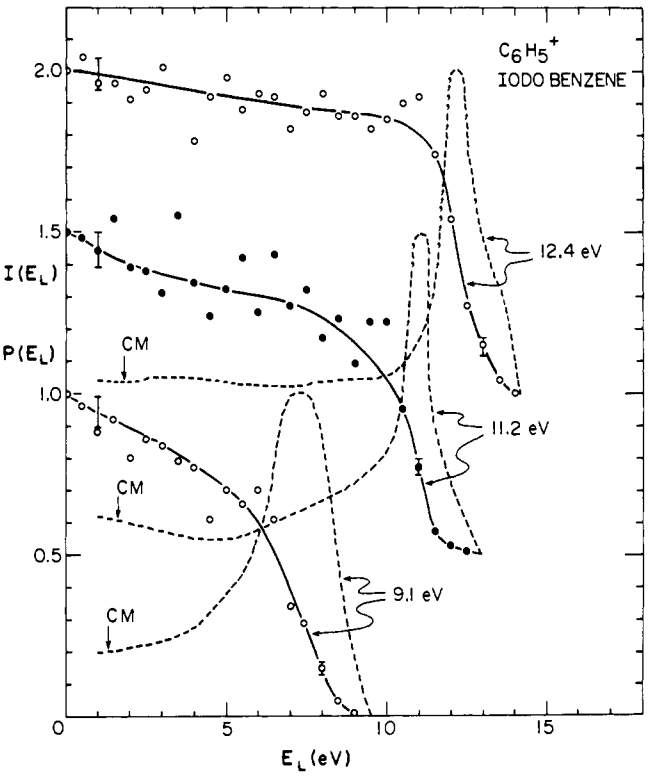

Figure 1. Stopping curves $I(E_L)$ (—) and their derivative energy distribution curves $P(E_L)$ (---) for the reaction with iodobenzene at the LAB angle of 5° for three different collision energies. The curves have been shifted for display, but are normalized to unity at $I(0)$ and at the maximum of $P(E_L)$. The energy a $C_6H_5^+$ would have moving at the speed of the CM is indicated by an arrow for each case. The error bars represent the statistical counting noise (~[counts]$^{1/2}$).

diagrams for $C_6H_5^+$ are shown in Figures 2 and 3 for the reaction with bromobenzene and nitrobenzene, respectively. In both of these the product ions are located almost exclusively with c.m. angles $0° \le \theta \le 90°$, i.e., in the direction of the initial Cs^+ c.m. velocity, and hence correspond to products scattered *backward* with respect to the *initial* C_6H_5X direction. These figures show that very little of the scattering is forward or even very near the center-of-mass (CM) of the system. In short, they both resemble very closely the kinematic map of the chlorobenzene reactive scattering reported earlier.[15]

One can already recognize this behavior from the LAB energy distributions at small LAB angles such as in Figure 1 for iodobenzene. From the $P(E_L)$'s at each of the three energies in this figure, one sees that most of the $C_6H_5^+$ ions have considerably greater energy than they would have moving at the speed of the CM; that is, their velocities are greater than the velocity of the CM. Hence, as in Figures 2 and 3 the scattered ions must appear on the kinematic map predominantly in the initial Cs^+ direction

(16) Simple considerations of the experiment reveal that the scattering must be symmetric about the Cs^+ velocity. That this is in fact true on this apparatus is shown and discussed in ref 11.

Table II. Center-of-Mass Energy Parameters[a]

organic reactant	E[b]	E_p'[c]	W_p'[c]	E_{max}'[d]	W_{min}'[d]	E_{max}'-(calcd)	W_{min}'-(calcd)[f]
C_6H_5Cl[e]	8.9	1.8	3.5	3.4	1.9	3.5	1.8
C_6H_5Cl[e]	11.3	3.6	4.1	5.7	2.0	5.9	1.8
C_6H_5Cl[e]	13.6	5.9	4.1	8.3	1.7	8.1	1.9
C_6H_5Br	8.9	3.1	2.3	4.9	0.5	4.7	0.7
C_6H_5I	9.1	3.2	2.5	4.7	1.0	4.7	1.0
C_6H_5I	11.2	5.4	2.4	6.8	1.0	6.8	1.0
C_6H_5I	12.4	5.9	3.1	7.5	1.5	7.9	1.1
$C_6H_5NO_2$	11.7	3.4	4.8	6.1	2.1	6.2	2.0

[a] All energies are in eV. The uncertainties in the measurement are estimated to be ±0.5 eV. [b] E is the *initial* relative kinetic energy, or collision energy; fwhm for E is 0.3 eV. [c] E_p' is the most probable energy from the product relative translational energy distribution at $\theta = 0°$. W_p' is the corresponding internal energy, $W_p' = E - \Delta H° - E_p'$. [d] E_{max}' is the largest relative recoil energy at $\theta = 0°$. W_{min}' is the corresponding internal energy, or residual energy; $W_{min}' = E - \Delta H° - E_{max}'$. [e] The results for C_6H_5Cl from ref 15 are included for comparison. [f] W_{min}' (calcd) $= E - \Delta H° - E_{max}'$(calcd).

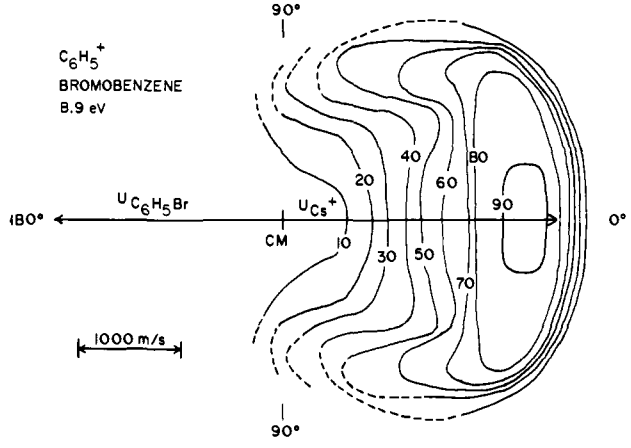

Figure 2. Cartesian center-of-mass contour diagram for the $C_6H_5^+$ product from bromobenzene. The length of the double arrow represents the initial Cs^+ LAB velocity, which because of the small C_6H_5Br (thermal) velocities is very nearly the relative velocity vector. The direction toward 180° is "forward" and that toward 0° is "backward" for C_6H_5Br with respect to the CM of the system. The dashed lines represent contours inferred from angular distribution data alone. The contours have been normalized to 100 at the maximum intensity (product ion flux).

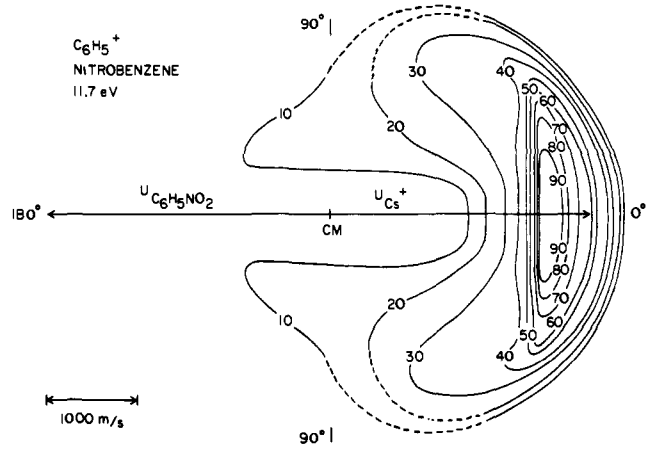

Figure 3. Cartesian center-of-mass contour diagram for the $C_6H_5^+$ product from nitrobenzene. The details of the diagram are as described in Figure 2.

and are thus *backward* scattered. (In comparison with a similar figure in ref 15 for chlorobenzene one finds considerably more scattering near the CM here. However, because of the mass differences the product ion fluxes at or near the CM in the iodobenzene case are rather uncertain.)

Because of this correspondence, the c.m. product translational energy distributions can be calculated directly and easily from the small angle LAB $P(E_L)$ curves for scattering in the *backward* direction.[17] Table II lists the collision energy E, and for each experiment the most probable product c.m. relative translational energy, E_p', and the maximum product relative translational energy, E_{max}', calculated from these curves. From these values and energy conservation one obtains also the most probable product internal energy, W_p', and the minimum product internal energy or residual energy, W_{min}', neglecting the small amount of thermal internal energy of the C_6H_5X molecules. These numbers are similarly included in Table II and are especially noteworthy, for it appears that they are roughly independent of collision energy for each reaction and that they seem to order the reactions into two groups: chlorobenzene and nitrobenzene on the one hand and bromobenzene and iodobenzene on the other. Interestingly, this same grouping appears in the phenyl cation AP's in Table I.

Mass scans were made at collision energies up to ~15 eV for secondary ion products which result from the fragmentation of excited $C_6H_5^+$. At these energies only $C_4H_3^+$ and a considerably smaller amount of $C_2H_3^+$ were observed. (The potential fragment $C_3H_3^+$ could not be detected because of the slight $^{39}K^+$ impurity in the Cs^+ beam.) Only the AP of $C_4H_3^+$ was measured (Table I).

Discussion

Three aspects of these results need to be discussed: the angular distributions and shape of the kinematic map, the energetics of the recoil energy distributions, and the nature of the secondary ion products.

A. Potential-Energy Surfaces and the Angular Distribution. The form of these chemical reactions is the attack by the Cs^+ ion on the covalent C_6H_5X molecule to yield the ionic Cs^+X^- and the phenyl cation. Because the electronic configuration of the Cs^+ remains essentially unchanged in the course of the reaction, one's attention can be focused on the evolution of C_6H_5X to $C_6H_5^+X^-$ under the influence of purely electrostatic (as opposed to "chemical") forces. Perhaps the best approach conceptually is to visualize this problem as a "curve crossing".[18]

For the purpose here it suffices to treat C_6H_5 as the single entity R. The reaction then takes place on two pseudotriatomic diabatic "slices" of the system's potential energy hypersurface, one corresponding to the interaction of Cs^+ with covalent RX and the other corresponding to the interaction of Cs^+ with ionic R^+X^-. These surfaces are shown schematically in Figure 4. The zero energy level is taken to be $Cs^+ + RX$ at large separations. On the covalent surface the large r_{CsX} and r_{RX} region is the separated atom plateau at the energy level of the homolytic dissociation, $D_0(R-X)$ which ranges from ~2.6 eV for iodobenzene to ~5.1 eV for fluorobenzene. The long-range force in the entrance "valley" is attractive due to the ion–rotationally averaged dipole and ion–induced dipole potentials, both $\sim 1/r^4$.[19] At smaller

(17) The values calculated here are "polar" not "Cartesian" coordinate fluxes. See the discussion in ref 11 and in references cited therein.

(18) See, for example: Child, M. S. "Molecular Collision Theory"; Academic Press: New York, 1974.

(19) Hirschfelder, J. O.; Curtiss, C. F.; Bird, R. B. "Molecular Theory of Gases and Liquids"; Wiley and Sons: New York, 1954, pp 984–986.

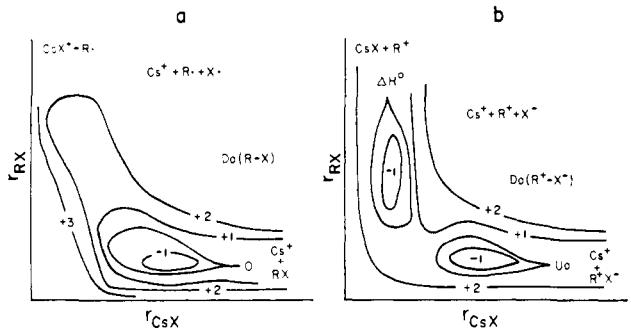

Figure 4. Pseudotriatomic potential energy surfaces for (a) $Cs^+ + RX$ and (b) $Cs^+ + R^+X^-$. In both cases the abscissa is the Cs–X distance r_{CsX} and the ordinate is the R–X distance r_{RX}. The potential energy is represented by contour lines as is customarily done. The shapes are intended to give a rough feeling for how each surface ought to vary with r_{CsX} and r_{RX}. The numbers given are arbitrary and just indicate the changes in the potential energy relative to the separated reactants and products. The shapes of the surfaces are also a function of the orientation angle.

separations the interaction is dominated by the ion–dipole potential, $U = qd_c\cdot\mathbf{r}/r^3$ (where q is the Cs^+ charge and d_c is the dipole moment of covalent RX), which depends on the orientation[20] as to whether it is attractive or repulsive. With the exception of CsI^+ which is only marginally stable (~0.1 eV) compared to $Cs^+ + I$, the CsX^+ molecules are unstable. Thus there is *no* exit valley on the covalent surface. (The mass scans did not reveal any species at the mass of CsI^+.)

The ionic diabatic surface is basically similar except that it is displaced upward in energy. At large r_{CsX} and r_{RX} values, the region becomes the separated ion plateau at energy level $D_0(R^+–X^-)$ which ranges from ~7.6 eV for nitrobenzene to ~10.4 eV for fluorobenzene.[21] The potential energy U_0 for equilibrium R^+X^- (and large r_{CsX}) can be roughly estimated by subtracting from $D_0(R^+–X^-)$ the Coulombic energy of attraction between R^+ and X^- at the RX equilibrium distance. These estimates for U_0 vary from ~3.0 eV for nitrobenzene to ~5.1 eV for fluorobenzene above the RX ground state. The potential energy in the excited entrance valley is as described above except that the R^+X^- dipole moment d_i is considerably greater than d_c. This surface does have an exit valley leading to the products $Cs^+X^- + R^+$, which should resemble the entrance valley since the electrostatic forces between the products are very similar to those between the reactants.

In this diabatic representation, the reactants start out on the covalent surface and the products emerge on the ionic surface. The critical region for the reaction is thus where the surfaces intersect, for it is there that a transition is possible. The probability for such a transition depends on the coupling of the surfaces, their shapes in the intersection region, and the relative velocity of the system through this region. Since little of this is known for the systems under study, attention is focused here strictly on the location and shape of the potential energy surfaces.

From the energetics presented for these reactions, it is clear that the reactant side of the ionic surface lies well above the covalent one except at small r_{CsX} or possibly in the entrance valley if the stronger ion–dipole forces of the ionic surface can compensate for the U_0 energy gap between RX and R^+X^-. For the most attractive case, the collisional orientation should be the linear $Cs^+–X–R$ one.[20] Considering only the strong ion–dipole potential, one finds the ionic surface will intersect the covalent one at

$$r_{int} = [q(d_i - d_c)/U_0]^{1/2} \quad (4)$$

Assuming that $d_i - d_c \approx 10$ D and $U_0 \approx 4$ eV, one obtains an intersection distance of 2.7 Å. Since the equilibrium CsX distances themselves are around 3 Å, it is obvious that the calculated intersection distance is too close for the ion–dipole approximation to be valid.[22] That is, for these systems the critical region for reaction must be in the repulsive zone at small r_{CsX} and r_{RX} values.

For the collisional orientation considered above, the force between reactants (and between products) is fairly strongly attractive except at close range. One might expect that the scattering would reflect this, namely, as in short-lived complexes, there should be a significant amount of forward scattering. The fact that there is essentially no forward scattering of products suggests that this orientation is not a favorable one for reaction. Rather, the more favorable orientations for reaction would appear to be closer to the "repulsive" ones in which the Cs^+ strikes the phenyl end of the RX molecule.

B. Ideal Knockout Model. A simple collision model which has been described previously[11,23] deals with just this situation. The Ideal Knockout Model (IKM) assumes that the endoergicity of the reaction must be overcome by E^*, the relative collision energy between Cs^+ and R^+, where

$$E^* = \tfrac{1}{2}m_{Cs}m_R V^2/m_{CsR} = Emm_R/m_{RX}m_{CsR} \quad (5)$$

where $m = m_{Cs} + m_R + m_X$, $m_{RX} = m_R + m_X$, and $m_{CsR} = m_{Cs} + m_R$. Relative to their center of mass, the recoil velocity of R^+ is

$$U^{*\prime} = [2m_{Cs}(E^* - \Delta H°)/m_R m_{CsR}]^{1/2} \quad (6)$$

and relative to the CM of the whole system, the R^+ recoil velocity is

$$U' = a\cos\theta + [(U^{*\prime})^2 - a^2\sin^2\theta]^{1/2} \quad (7)$$

where $a = (m_X m_{Cs}/mm_{CsR})V$ and $\theta = 0°$ for backward scattered R^+. The relative translational energy, or recoil energy,

$$E' = \tfrac{1}{2}m_R m(U')^2/m_{CsX} \quad (8)$$

Since E^* must be at least equal to $\Delta H°$, the IKM also predicts appearance potentials.

Thus, from the measured AP's for reaction 2 one can calculate its $\Delta H°$ from eq 5 and 6, using E = AP. These heats of reaction are listed under $\Delta H°_{calcd}$ (eq 2) in Table I, and are then employed in equations 6–8 for each collision energy E to give an E' which should be the largest possible recoil energy. These values are listed in Table II under E_{max}'(calcd). The agreement here is *excellent* in *all* cases. The only real disagreement is seen in Table I where the calculated heats of reaction for chloro- and nitrobenzenes are ~1 eV larger than the expected values.

The reason for the extra energy in $\Delta H°$ in the chlorobenzene and nitrobenzene reactions is unclear. One possibility for the latter compound is that NO_2^- is produced in an electronically excited state. However, Okada has shown in energy loss collision studies[24] that the lowest excited states of NO_2^- are $^3B_1$ (2.9 eV), $^3B_2$ (3.4 eV), and $^1B_1$ (3.7 eV). Another possibility is that the phenyl cation produced with X = Cl or NO_2 is in an excited state. However, the reported calculations[2] show only triplet states in this energy region. Because the reactants are singlets, one expects the operative surfaces to be singlet surfaces unless there is strong spin–orbit coupling. In fact, the spin–orbit coupling in Br and I is known to be strong,[25] and one might have expected that if a triplet product were produced it would occur in the X = Br or I cases. So unless the ordering found in these calculations is in error, triplet lying below singlet, this explanation does not seem likely.

(20) The relative velocity in these experiments is roughly 5000 m/s = 50 Å/ps. Thus, the Cs^+ and RX molecules at 10 Å apart reach a separation of 5 Å in $\sim 10^{-13}$ s. In this period the RX molecule will have vibrated and rotated very little so that one can speak of a collision with a fixed orientation. These orientations are, of course, randomly distributed.

(21) $D_0(R^+–X^-) = D_0(R–X) + IP(R) - EA(X)$. The ionization potential of C_6H_5 is 8.8 eV (see ref 4) and the electron affinities for X range from 3.1 eV for I to 4.0 eV for NO_2 (see ref 8, p E-55).

(22) A similar calculation for benzyl chloride has r_{int} = 4.1 Å and for *tert*-butyl chloride r_{int} = 9.1 Å.

(23) Miller, G. D.; Safron, S. A. *J. Chem. Phys.* **1976**, *64*, 5065–5072. The formula given there for a has a factor of m_{Cs} left off.

(24) Okada, S. *Chem. Phys.* **1979**, *41*, 423–429.

(25) Turro, N. J. "Molecular Photochemistry"; W. A. Benjamin: New York, 1967.

It is known that opening of the benzene and phenyl rings requires about 1 eV.[26] Thus, it is possible that the $C_6H_5^+$ observed in reaction with X = Cl and NO_2 is a linear species rather than phenyl. However, why this should not also occur for X = Br and I is not clear, and makes this explanation unconvincing. A fourth and most reasonable possibility is that the intersection regions for chlorobenzene and nitrobenzene are somewhat more repulsive than for bromobenzene and iodobenzene, possibly because they are better shielded from Cs^+ by the phenyl group. In short, for the former pair there is an activation energy of ~1 eV.

An interesting and speculative extension of the IKM is to calculate from eq 6 and 8 the energy that must be absorbed in order to have the recoil energy equal to the most probable relative translational energy E_p' (Table II). The results are 6.1, 6.7, and 6.7 eV for the three chlorobenzene experiments; 7.0 eV for nitrobenzene; 4.6 eV for bromobenzene; and 4.3, 4.3, and 4.8 eV for iodobenzene. These values average 1.6 eV above the IKM calculated $\Delta H°$ values. The quantum calculations[2] on the singlet phenyl ion show that the hexagonal or benzenelike structure is vibrationally excited by roughly 1 eV relative to the more stable "distorted" geometry. The fact that the angular distributions are highly asymmetric implies that the reaction time is very fast, possibly on the order of vibrational periods.[20] Hence, it is suggestive that the most probable recoil energy arises from collisions which absorb the $\Delta H°$ plus the ring "distortion" energy, the products departing before relaxation can occur.

C. Fragmentation. If the formation of $C_4H_3^+$ takes place in a two-step process as given by reactions 2 and 3, then its AP may also be calculated from the IKM since the required extra energy of reaction 3 would have to be deposited in $C_6H_5^+$.

As was done previously, one can also use the model to calculate the reaction $\Delta H°$ from its measured AP. These calculated $\Delta H°$'s are included in Table I under $\Delta H°_{calcd}$ (eq 2 + 3). The difference of the calculated $\Delta H°$'s, $\Delta H°_{calcd}$ (2 + 3) − $\Delta H°_{calcd}$ (eq 2), yields the values 2.5, 2.7, 2.9, and 3.1 eV for chloro-, bromo-, iodo-, and nitrobenzene, respectively. The average 2.8 eV is well within the experimental uncertainty for each measurement, and implies that the $\Delta H°$ for reaction 3 is 1.3 eV less than expected, or that the $\Delta H°_f(C_4H_3^+)$ = 12.0 eV (276 kcal/mol) rather than the reported 13.3 eV (307 kcal/mol).[10] Moreover, since the differences taken above are between calculated $\Delta H°$'s, the ~1 eV activation energy (or extra energy) for $C_6H_5^+$ formation from reaction 2 for chloro- and nitrobenzene still appears in the $C_4H_3^+$ formation. This suggests that this extra energy resides in the newly formed CsCl or $CsNO_2$ molecules rather than remaining in the $C_6H_5^+$ ion as vibrational energy as it does not appear to be available for fragmentation. (Also, see below).

The IKM predicts that when an amount of energy $\Delta H° + W$ is absorbed in the collision between Cs^+ and $C_6H_5^+$, the recoil energy E' can be calculated by replacing $\Delta H° + W$ for $\Delta H°$ in eq 6. By considering the relative motion between the rebounding Cs^+ and the unchanged X^-, the model also predicts that vibrational energy in CsX is $W_{CsX'} = E - E' - \Delta H° - W$. Thus, for example, from Figure 3, a backward scattered $C_6H_5^+$ with c.m. velocity of 1500 m/s has E' = 1.3 eV, and, according to the model, $\Delta H° + W$ = 8.5 eV and $W_{CsX'}$ = 1.9 eV. Taking $\Delta H°$ to be the IKM calculated value of 4.6 eV, one finds W = 3.9 eV. If one takes the IKM literally, then this 3.9 eV should be the internal energy of $C_6H_5^+$ and is well above the 2.8 eV necessary to fragment $C_6H_5^+$ to $C_4H_3^+$ and C_2H_2. Such ions are predissociative in that they should have sufficient energy to dissociate, but apparently in the time needed to reach the detector (~10^{-4} s) they do not fragment. If this situation actually obtains, it suggests that the secondary ion products come from electronically excited rather than vibrationally excited phenyl ions.[27]

The possible fragmentation reactions of $C_6H_5^+$ in collision energies up to 15 eV include[28]

$$C_6H_5^+ \rightarrow C_4H_4^+ + C_2H \quad (6.1\text{ eV}) \qquad (9)$$

$$C_6H_5^+ \rightarrow C_4H_3^+ + C_2H_2 \quad (4.1\text{ eV}) \qquad (10)$$

$$C_6H_5^+ \rightarrow C_4H_2^+ + C_2H_3 \quad (5.9\text{ eV}) \qquad (11)$$

$$C_6H_5^+ \rightarrow C_3H_3^+ + C_3H_2 \quad (4.9\text{ eV}) \qquad (12)$$

$$C_6H_5^+ \rightarrow C_3H_2^+ + C_3H_3 \quad (7.6\text{ eV}) \qquad (13)$$

$$C_6H_5^+ \rightarrow C_2H_3^+ + C_4H_2 \quad (4.6\text{ eV}) \qquad (14)$$

$$C_6H_5^+ \rightarrow C_2H_2^+ + C_4H_3 \quad (6.9\text{ eV}) \qquad (15)$$

With the exception of $C_3H_3^+$ which as mentioned could not be detected in these experiments, the only ions observed were $C_4H_3^+$ and $C_2H_3^+$. These are even-electron species. Hence the even–even rule, where the even-electron $C_6H_5^+$ forms only the even-electron products, appears to hold here.[29] A similar result was also noted previously.[11,12,23]

Conclusions

A. The angular and energy distributions observed for the reactions reported here suggest that the phenyl cation is formed as a result of a "hard" collision with Cs^+.

B. The Ideal Knockout Model which assumes that the interaction between Cs^+ and C_6H_5X is primarily the repulsion between the Cs^+ and $C_6H_5^+$ appears to provide a consistent energetic description of the reaction processes.

C. The fits of the model to the data suggest that the reactions of Cs^+ with chloro- and nitrobenzene have activation energies (above the reaction endoergicities) of ~1 eV, while those with bromo- and iodobenzene do not. In addition, the model finds that the $\Delta H°_f(C_4H_3^+)$ = 12.0 eV (276 kcal/mol), about 1.3 eV less than the previously reported value.

D. The energy distributions also imply that the fragmentation occurs as the result of electronic excitation of the $C_6H_5^+$ ion rather than just vibrational excitation of the ground state, and that these systems may be models for studies of predissociation in polyatomic systems.

E. These results taken together with previous work in this laboratory show that not only is there a direct correlation between solution experiments and scattering experiments, but also that scattering experiments can provide the complementary dynamical information necessary to achieve a complete understanding of reactions in solutions.

Acknowledgment. The authors wish to thank the Research Corporation for partial support of this research. The authors are also grateful to the referees for some helpful suggestions.

(26) See, for example: Rosenstock, H. M.; Larkins, J. T.; Walker, J. A. *Int. J. Mass Spectrom. Ion Phys.* **1973**, *11*, 309–328 and references cited therein.

(27) Dissociation of $C_6H_6^+ \rightarrow C_4H_4^+$ is proposed to occur from a state 2.25 eV above the ground state of $C_6H_6^+$, see ref 26.

(28) These reactions energies, including that for $C_4H_3^+$, are based on values in ref 10.

(29) For example, see: McLafferty, F. W. *Org. Mass Spectrom.* **1980**, *15*, 114–121.